*Biochimica et Biophysica Acta*, 470 (1977) 303—316


BBA 77817

# LATERAL PHASE SEPARATIONS IN BINARY MIXTURES OF PHOSPHOLIPIDS HAVING DIFFERENT CHARGES AND DIFFERENT CRYSTALLINE STRUCTURES

ELIZABETH J. LUNA and HARDEN M. McCONNELL *

*Stauffer Laboratory for Physical Chemistry, Stanford University, Stanford, Calif. 94305 (U.S.A.)*

(Received February 2nd, 1977)

## Summary

Synthetic dipalmitoyl phosphatidylserine exhibits a sharp chain-melting transition temperature at 51° C as judged by partitioning of the spin label 2,2,6,6-tetramethylpiperidine-1-oxyl. Phase diagrams representing lateral phase separations in binary mixtures of dipalmitoyl phosphatidylserine with dipalmitoyl phosphatidylcholine as well as with dimyristoyl phosphatidylcholine are derived from paramagnetic resonance determinations of 2,2,6,6,-tetramethylpiperidine-1-oxyl partitioning, freeze-fracture electron microscopic studies and theoretical arguments that limit the general form of acceptable phase diagrams. The reported phase diagrams are the first to describe binary mixtures in which one lipid is charged and the second lipid uncharged. These phase diagrams also are the first to include the problem of solid phases with different crystalline conformations as it relates to the occurrence of a pretransition in phosphatidylcholines and its absence in phosphatidylserines. In addition to the phase diagrams reported here for these two binary mixtures, a brief theoretical discussion is given of other possible phase diagrams that may be appropriate to other lipid mixtures with particular consideration given to the problem of crystalline phases of different structures and the possible occurrence of second-order phase transitions in these mixtures.

## Introduction

There is great current interest in lateral phase separations in mixtures of phospholipids wherein some lipid components are charged and the other lipid components are uncharged. This is because in such mixtures the occurrence and/

* To whom correspondence should be addressed.
Abbreviations: TEMPO, 2,2,6,6-tetramethylpiperidine-1-oxyl.

or degree of lateral phase separation can be triggered or modulated isothermally by water-soluble components such as calcium ion [1—6], hydrogen ion [2,4], polypeptides [6-7], etc. Lateral phase separations in lipid vesicular structures can lead to enhanced membrane permeation of water-soluble substances [8—12] and reorganization of membrane components [13—15] as well as membrane fusion [16]. The latter is of interest not only in connection with naturally occurring biological fission and fusion processes, but also in connection with the possibility of artificially introducing genetic material and enzymes into cells. In spite of these attractive features of mixtures of charged and uncharged lipids, no qualitative or quantitative phase diagrams representing lateral phase separations in these mixtures have been published. The present work describes two approximate phase diagrams for binary mixtures of dipalmitoyl phosphatidylserine with dipalmitoyl phosphatidylcholine and with dimyristoyl phosphatidylcholine. These phase diagrams are approximate, based on TEMPO binding, freeze-fracture electron microscopic data and theoretical arguments concerning acceptable forms for such phase diagrams. The reported phase diagrams are also of special interest in that they take into account problems arising when the low temperature solid crystalline phases of the two lipids have different crystalline structures. Since these special structural problems may be significant for other mixtures of lipids, additional discussion of other possible phase diagrams for lipid mixtures are briefly considered from a theoretical point of view.

*Notations for structures of lipid phases*

The symmetries and molecular structures of various lamellar phases of phospholipids have been studied extensively. Throughout the present paper we use the notations introduced by Luzzati and colleagues for various lipid phases, i.e., $L_\alpha$, $L_{\beta'}$, $P_{\beta'}$ [17]. Here L represents a lamellar state of the lipid bilayers, $\alpha$ represents states of the fatty-acid hydrocarbon chains that are "fluid" or liquid-like, and $\beta'$ represents a state in which the fatty chains are predominantly in their extended, all-*trans* conformation and are tilted relative to the normal to the bilayer planes. The symbol P refers to a monoclinic structure, in this case one in which the molecules in each bilayer do not lie in a single plane, but are located in bilayers that have a periodic, wavelike, undulating pattern, sometimes described as "bands". The repeat periods in these banded structures for typical phosphatidylcholines are in the range 120—500 Å. In the present paper the notations $L_\alpha$, $L_{\beta'}$, and $P_{\beta'}$ refer to multilamellar arrays of lipid bilayers that exactly, or approximately, fall in the category of smectic liquid crystals or lamellar crystals. All of our work deals with such systems, i.e., multilamellar liposomes. However, from a biological point of view one is more directly concerned with the properties of single bilayers. In recent unpublished work we have observed "bands" characteristic of the $P_{\beta'}$ phase of phosphatidylcholines in large (diameters of about 1 $\mu$m) single compartment vesicles using freeze-fracture electron microscopy. Thus it is likely that there is a one-to-one correspondence between the $L_\alpha$, $P_{\beta'}$, and $L_{\beta'}$ phases of multilamellar liposomes and corresponding phases in isolated single bilayer membranes.

There is strong evidence that the chain-melting transition $P_{\beta'} \longleftrightarrow L_\alpha$ in dimyristoyl phosphatidylcholine (at 23°C) and in dipalmitoyl phosphatidylcholine (at 41°C) is first-order; the transitions are associated with substantial

changes in enthalpy ($\Delta H$) and volume ($\Delta V$) [18—20]. There is evidence that the "pretransition" in phosphatidylcholines is also first-order, there being a reported $\Delta H$ of transition [20], as well as extensive evidence for hysteresis in this transition [21,22] (not possible for second-order transitions [23]).

In contrast to the two phosphatidylcholines considered here there is, as shown below, no evidence for a pretransition (corresponding to $L_\beta$ or $L_\beta' \leftrightarrow P_\beta'$) nor for a banded phase of structure $P_\beta'$ in the case of dipalmitoyl phosphatidylserine. Thus, not only are there differences in charges between the phosphatidylcholine and phosphatidylserine molecules, but there are also significant differences in the structure of some of their crystalline phases. The significance of such structural differences in terms of phase diagrams will also be evident in the subsequent discussion.

## Materials and Methods

### *Materials*

Dimyristoyl phosphatidylcholine and dipalmitoyl phosphatidylcholine were purchased from Calbiochem and were used without further purification. TEMPO was provided by Dr. Wolfgang Kleemann.

L-α-dipalmitoyl phosphatidylserine was synthesized by the method of Baer and Maurukas [24]. Complete purification of the intermediate, dipalmitoyl, L-α-glyceryl-phenylphosphoryl *N*-carbobenzoxy-L-serine benzyl ester, was achieved by elution from a Bio Sil A (200—325 mesh) column with a chloroform-methanol gradient. Hydrogenation, trituration and recrystallization resulted in a fine white powder containing a small (≈2%) impurity which was removed by a second silicic acid column. Centrifugation (27 000 × *g*, 15 min, 20° C) cleared contaminating silicic acid from a solution of dipalmitoyl phosphatidylserine in 30 : 1 chloroform/acetic acid. In each of several different solvent systems the final product formed one spot on silica gel thin-layer chromatography. The compound stained for carbon, phosphorus, and serine and co-migrated with bovine brain phosphatidylserine (Schwarz/Mann). L-α-Dipalmitoyl phosphatidylserine had m.p. = 153—155° C, $[\alpha]_D^{20}$ = + 17.7 ± 0.8° C (*c* 1 in benzene) (Found: C, 61.9; H, 10.0; N, 1.9; P, 4.1. Calculated for $C_{38}H_{74}O_{10}NP$: C, 62.0; H, 10.1; N, 1.9; P, 4.2%). Negative specific rotations approximately the same as those reported for L-α-distearoyl phosphatidylserine by Baer and Maurukas [24] were obtained after incubation at temperatures above 65° C, but analysis by thin-layer chromatography showed the appearance of a second compound in these samples.

### *Phospholipid dispersions*

Dimyristoyl and dipalmitoyl phosphatidylcholine were stored as 1% ethanolic solutions; dipalmitoyl phosphatidylserine was kept in solid form until shortly before use when 5—10 mg were dissolved per ml of warm (50—55° C) chloroform. After equilibration to room temperature, lipid concentrations were verified by assaying aliquots of the stock solutions for phosphate by the method of McClare [25]. The chloroform-ethanol solution which contained 5—7 μmol of the desired lipids was evaporated under vacuum to dryness. The lipids were then re-dissolved in excess warm chloroform and again evaporated to dryness

under vacuum. A glass bead, 5 μl of a 0.01 M TEMPO solution, and about 85 μl of 0.2 M sodium phosphate buffer containing 1.0 mM EDTA, pH 7.2, were then added to the 5 or 10 ml flask. The lipids were dispersed by vortexing at 55—60°C for several minutes and allowed to settle for 1—2 h before transfer to a 50 μl capillary pipet used as a sample cell for electron paramagnetic resonance measurement. The bulk pH of these dispersions was 6.9 or higher both before and after heating to 65°C. Final lipid concentrations were approximately 5% by weight.

Samples for freeze-fracture electron microscopy were prepared as described for the magnetic resonance experiments except TEMPO was omitted from the aqueous dispersions. Usually, one chloroform-ethanol solution was made for a given lipid mixture and was divided appropriately into samples for ESR experiments and freeze-fracture electron microscopy.

*Paramagnetic resonance spectroscopy*

All measurements were made on a Varian E-12 spectrometer at X-band with the sample cell oriented horizontally to minimize the settling of the phospholipid liposomes. The sample cell holder and temperature control accessories described by Gaffney [26] were used to insure reproducible sample insertion and accurate temperature control. The temperature was measured with a copper-constantan thermocouple connected to a Smith-Florence potentiometric microvoltmeter. Spectral parameters were measured for both heating and cooling of the sample at rates of 5—10°C per hour.

*Freeze-fracture electron microscopy*

Samples cooled to the quench temperature were obtained by heating a beaker of water above the transition temperature of the lipid and then allowing it to cool naturally. To minimize evaporation, samples to be heated to the quench temperature were kept on ice until 1—2 μl droplets were pipetted onto copper planchets resting on a metal block at the desired temperature in a room thermostatted to within 1—2 degrees of this temperature. After equilibration for 2—3 min, the samples were quenched and replicated as described previously [22]. Micrographs were taken on 3¼″ × 4″ Kodak electron microscope film with an initial magnification of 33 000× in a Hitachi HU-11E electron microscope.

## Results

*Phase transition of dipalmitoyl phosphatidylserine*

The spin label molecule TEMPO is readily soluble in water and in phospholipid bilayers in the fluid, liquid-crystalline state but is excluded from bilayers in the solid or gel phase. The TEMPO spectral parameter, $f$, defined as $H/(H + P)$ (Fig. 1) is roughly proportional to the fraction of the lipid which is in the fluid state [27]. Plots of the TEMPO solubility parameter $f$ vs. $T$, or $1/T$, have been used to determine phase diagrams for saturated [28] and unsaturated [29] phospholipids. Here we have applied this technique to the measurement of the transition temperature of the charged lipid, dipalmitoyl phosphatidylserine, dispersed in excess aqueous buffer. A plot of the TEMPO spectral

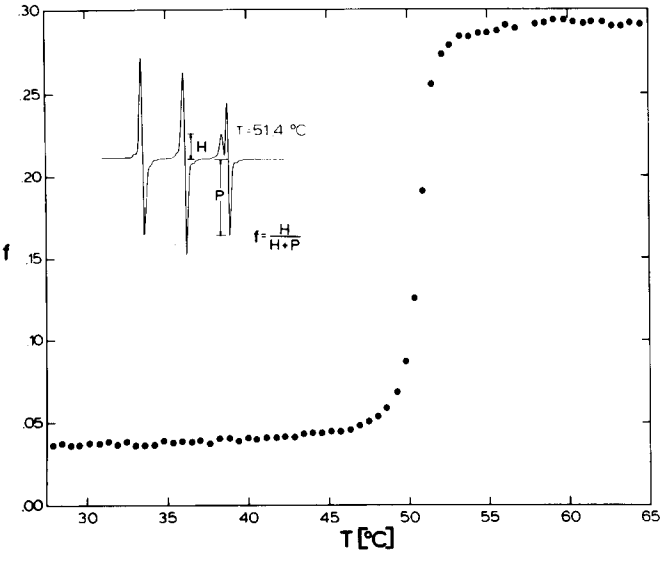


Fig. 1. The TEMPO spectral parameter, $f$, vs. temperature for an aqueous dispersion of ionized dipalmitoyl phosphatidylserine (50 mg/ml). $H$ is approximately proportional to the amount of spin label dissolved in the membrane bilayer and $P$ is proportional to the amount observed in the aqueous region [39].

parameter, $f$, as a function of temperature for this lipid is illustrated in Fig. 1. Dipalmitoyl phosphatidylserine has a transition temperature of 50.8°C, defined as the average value of the beginning and the completion temperatures of the TEMPO transition curve (49.5—52.0°C). This value is in good agreement with the result obtained previously by MacDonald et al. [30]. Using differential scanning calorimetry, these workers observed a broad transition centered at about 53°C for fully ionized dipalmitoyl phosphatidylserine at a concentration of 25—100 mg/ml.

*Spin-label and freeze-fracture data on binary mixtures*

Fig. 2A gives illustrative plots of the TEMPO spectral parameter as a function of temperature for binary mixtures of dipalmitoyl phosphatidylserine and dimyristoyl phosphatidylcholine. Each of these curves has two major abrupt changes of slope; such changes have generally been interpreted as the onset and completion of lateral phase separations [28,29], particularly when agreement with freeze-fracture electron microscopic data is obtained [31,32]. These transition temperatures are determined from the intersections of lines drawn through the three main regions of each curve. This procedure is shown for the 90 mol% dipalmitoyl phosphatidylserine curve in Fig. 2A. A phase diagram derived from these straight line intersections is presented in Fig. 2B, where S refers to a solid, crystalline (or "gel") phase and F refers to a fluid ($L_\alpha$) state.

The dimyristoyl phosphatidylcholine-dipalmitoyl phosphatidylserine phase diagram illustrated in Fig. 2B is a simple solid-solution, fluid-solution phase diagram that describes a two-dimensional equilibrium between a fluid phase and a solid phase. However, we can be certain that the complete phase diagram for this lipid mixture cannot be this simple. In the first place, both phase transi-

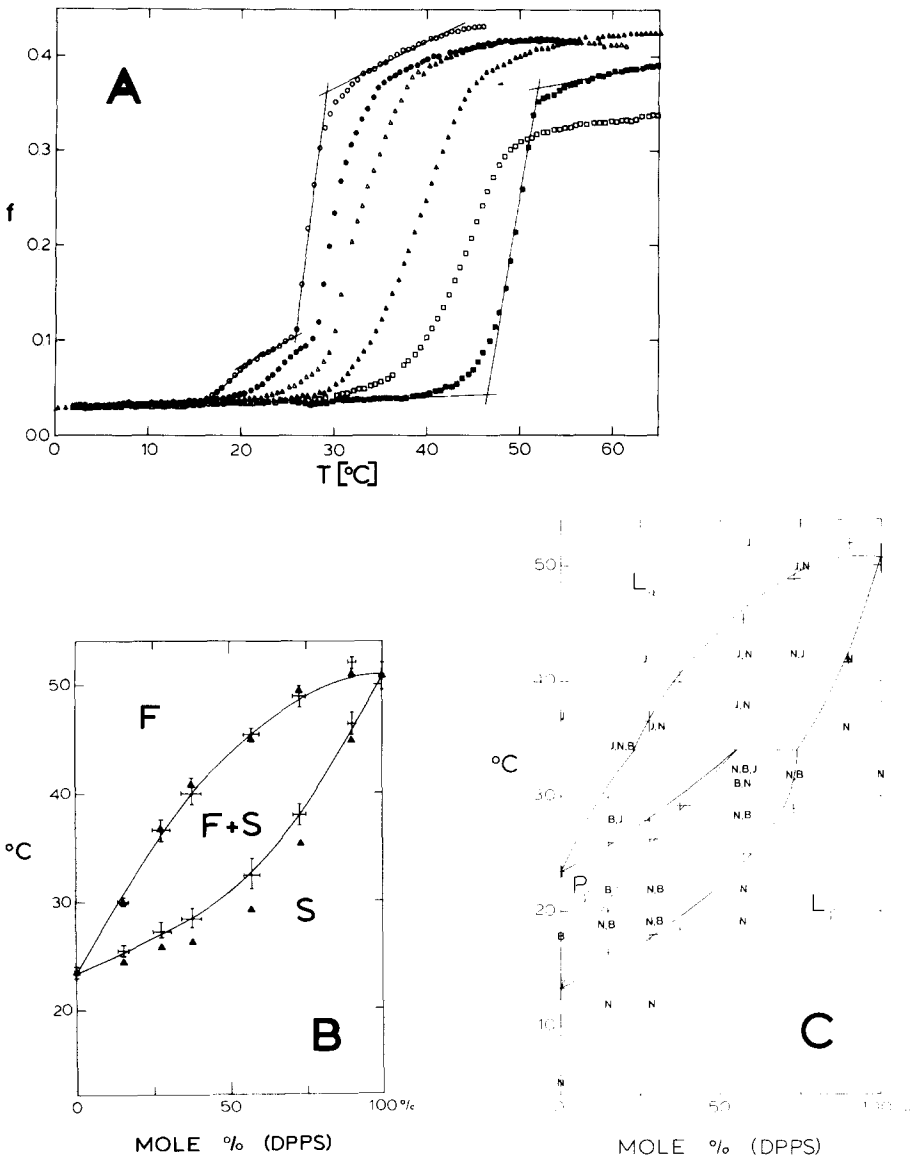


Fig. 2. (A), experimental TEMPO spectral parameter, $f$, as a function of temperature for aqueous suspensions of dimyristoyl phosphatidylcholine containing: (○), 15 mol%; (●), 27 mol%; (△), 37 mol%. (▲), 57 mol%; (□), 73 mol%. (■), 90 mol% dipalmitoyl phosphatidylserine. (B), traditionally-obtained phase diagram for aqueous dispersions of the dimyristoyl phosphatidylcholine-dipalmitoyl phosphatidylserine binary system: temperature vs. mol fraction of dipalmitoyl phosphatidylserine (DPPS). (⧺), data taken as described in the text from temperature breaks of experimental TEMPO spectral parameter heating curves in Fig. 2A; (▲), data taken from the temperature breaks of experimental spectral parameter cooling curves showing the 1—2°C hysteresis typical of charged phospholipids [30,40]. (C), complete phase diagram for aqueous dispersions of binary mixtures of dimyristoyl phosphatidylcholine and dipalmitoyl phosphatidylserine. (+), Data obtained from well-defined temperature breaks of the TEMPO spectral parameter heating curves by the procedure shown for 15 mol% dipalmitoyl phosphatidylserine (DPPS) in Fig. 2A. Hystereses similar to those shown in Fig. 2B were observed but, for the sake of clarity, only data from heating curves are presented. J, N and B denote the presence of jumbled, smooth and banded textures on fracture faces of samples quenched from the designated locations on the phase diagram. The regions of the phase diagram containing $L_\alpha$ phase only, $P_\beta'$ phase only and $L_\beta'$ phase only are indicated.

tions in the phosphatidylcholine are not represented on the diagram. In the second place, there must be some temperature-composition path on the phase diagram where one proceeds from a banded $P_{\beta'}$ phase of dipalmitoyl phosphatidylcholine to a non-banded crystalline phase (e.g., $L_{\beta}$ or $L_{\beta'}$) of dipalmitoyl phosphatidylserine. The nature of the phase boundaries that this path must cross is totally unspecified by the diagram in Fig. 2B.

Armed with the knowledge that the phase diagram under discussion must be more complex than the one depicted in Fig. 2B, we have re-examined the TEMPO binding curves shown in Fig. 2A, looking for well-defined break points. In some cases, the presence of additional break points is obvious, such as those seen for lipid compositions of 15 mol% and 27 mol% dipalmitoyl phosphatidylserine. In other cases, break points are reassigned. Break points in the data in Fig. 2A that are, in our opinion, rather well-defined are indicated by crosses (+) in Fig. 2C.

A wide temperature-composition region in Fig. 2C was also examined using freeze-fracture electron microscopy. Fig. 3 exhibits examples of freeze-fracture electron micrographs of mixtures of dipalmitoyl phosphatidylserine in dimyristoyl phosphatidylcholine corresponding to widely different temperature-composition points. Samples quenched from temperatures above the highest temperature breaks in the TEMPO parameter curves have smooth patches and jumbled lines on their fracture faces with the amount and degree of jumbling dependent on the quenching rate of the sample [33] and on the phosphatidylserine concentration (Fig. 3a and 3b). This appearance is characteristic of rapidly-quenched fluid phosphatidylcholines [33,34] and is denoted in Fig. 2C by the letter "J". Samples quenched from temperatures below the lowest TEMPO parameter curve breaks exhibit smooth fracture surfaces which are occasionally marked by random, widely-spaced "lines" (Fig. 3h). The letter "N" is used to designate the points on the phase diagram at which this smooth texture is observed. Regular band patterns are observed on fracture faces of samples containing low concentrations of phosphatidylserine when these samples are quenched from intermediate temperatures. In Fig. 2C, "B" denotes the presence of periodic bands such as those displayed in Fig. 3g.

When two textures are observed on the fracture surfaces of a sample, this fact is recorded at the appropriate point on the temperature-composition diagram by listing both designating letters with the first letter denoting the predominant texture. Examples of coexisting jumbled and smooth textures are presented in Figs. 3c and 3d. Coexisting jumbled and banded fracture surfaces are seen in Fig. 3e while Fig. 3f shows both banded and smooth textures.

The TEMPO spectral parameter curves for binary mixtures of dipalmitoyl phosphatidylcholine and dipalmitoyl phosphatidylserine are given in Fig. 4A; break points in the data in Fig. 4A are indicated by crosses (+) in Fig. 4B. Fig. 5 exhibits freeze-fracture electron micrographs of mixtures of dipalmitoyl phosphatidylserine in dipalmitoyl phosphatidylcholine. The jumbled texture (denoted by "J" on Fig. 4B) becomes less noticeable with increasing concentrations of phosphatidylserine (Fig. 5a and 5b) until it disappears altogether at about 75 mol% phosphatidylserine (Fig. 5c). Similar smooth fracture surfaces are observed for all samples quenched from temperatures below the lowest breaks in the TEMPO parameter curves of Fig. 4A. Fig. 5g presents an example

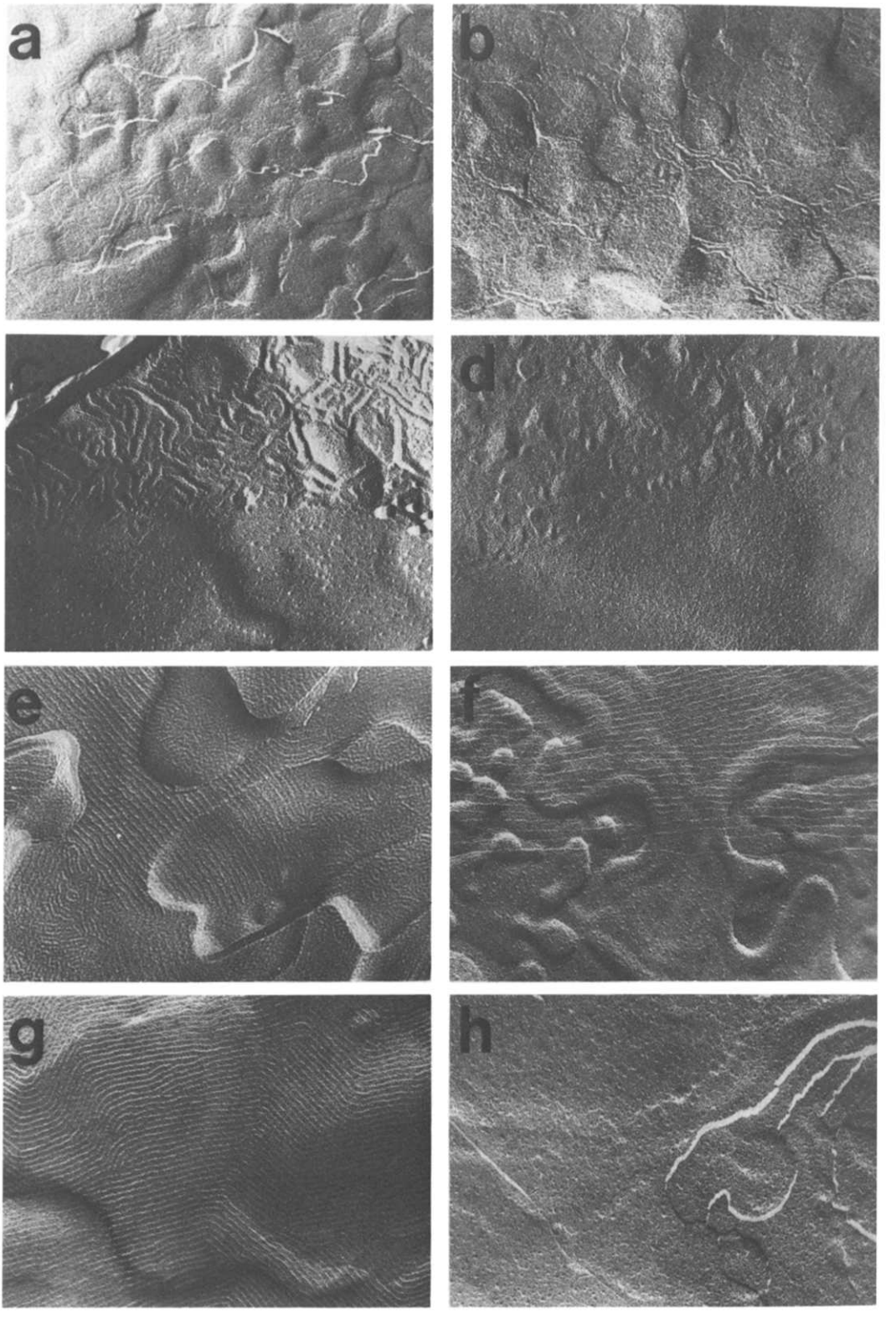
a
b
d
e
f
g
h

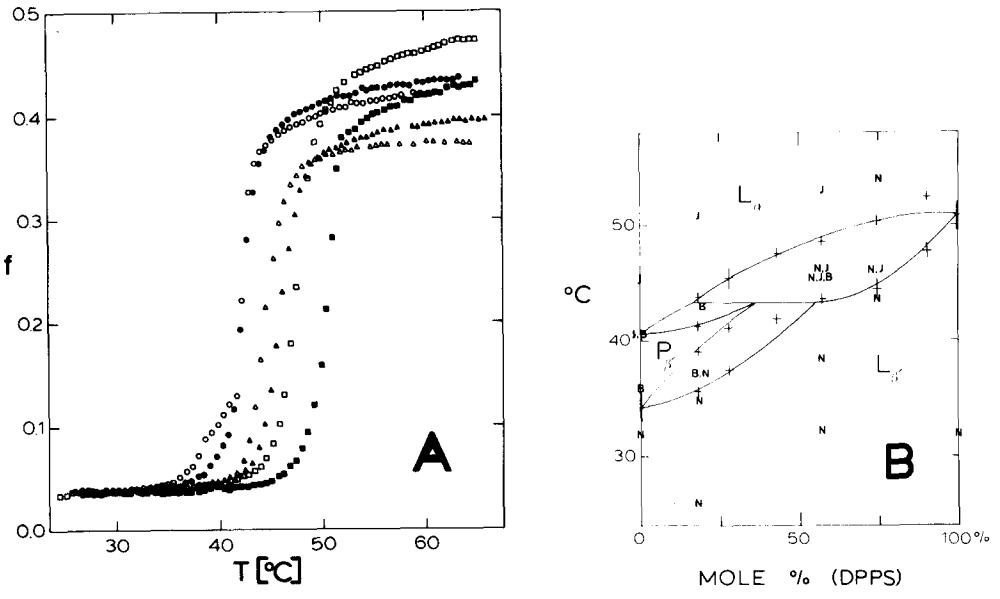


Fig. 4. (A), experimental TEMPO spectral parameter as a function of temperature for aqueous suspensions of dipalmitoyl phosphatidylcholine containing: (○), 18 mol%; (●), 28 mol%; (△), 43 mol%; (▲), 57 mol%; (□), 75 mol%; (■), 90 mol% dipalmitoyl phosphatidylserine. (B), complete phase diagram for aqueous dispersions of the dipalmitoyl phosphatidylcholine-dipalmitoyl phosphatidylserine binary system: temperature vs. mole fraction of dipalmitoyl phosphatidylserine. (+), data taken from temperature breaks of experimental TEMPO spectral parameter heating curves in Fig. 5A. Cooling curves showed 1—2°C hystereses of the lower break temperatures; for the sake of clarity, only heating data are presented. J, N and B denote the presence of jumbled, smooth and banded textures on fracture faces of samples quenched from the designated locations on the phase diagram. The regions of the phase diagram containing $L_\alpha$ phase only, $P_\beta'$ phase only and $L_\beta'$ phase only are indicated.

of a smooth-textured fracture face designated by "N" on Fig. 4B. Coexisting jumbled and smooth textures (Fig. 5e) are observed on fracture surfaces of samples quenched from the region of the dipalmitoyl phosphatidylcholine-dipalmitoyl phosphatidylserine phase diagram which is postulated to consist of coexisting $L_\alpha$ and $L_\beta'$ phases. Similarly, both banded ("B") and smooth fracture faces are observed (Fig. 5f) when samples are quenched from the region of the phase diagram in which we expect to find coexisting $P_\beta'$ and $L_\beta'$ phases. (See Discussion.) In drawing the phase diagrams in Figs. 2C and 4B we assumed that the low temperature phase of dipalmitoyl phosphatidylserine has the structure $L_\beta'$. In the following discussion consideration is given to the possibility that the structure may not be $L_\beta'$.

Fig. 3. Freeze-fracture electron micrographs of aqueous dispersions of dimyristoyl phosphatidylcholine-dipalmitoyl phosphatidylserine mixtures. Mol% dipalmitoyl phosphatidylserine and quench temperature are as follows: a, 27%, 42°C; b, 57%, 52°C; c, 57%, 38°C; d, 57%, 42°C; e, 15%, 28°C; f, 27%, 22°C; g, 15%, 22°C; h, 27%, 12°C. All samples were heated to the quench temperatures which are accurate to ±2—3°C. Magnifications are about 44 000X.

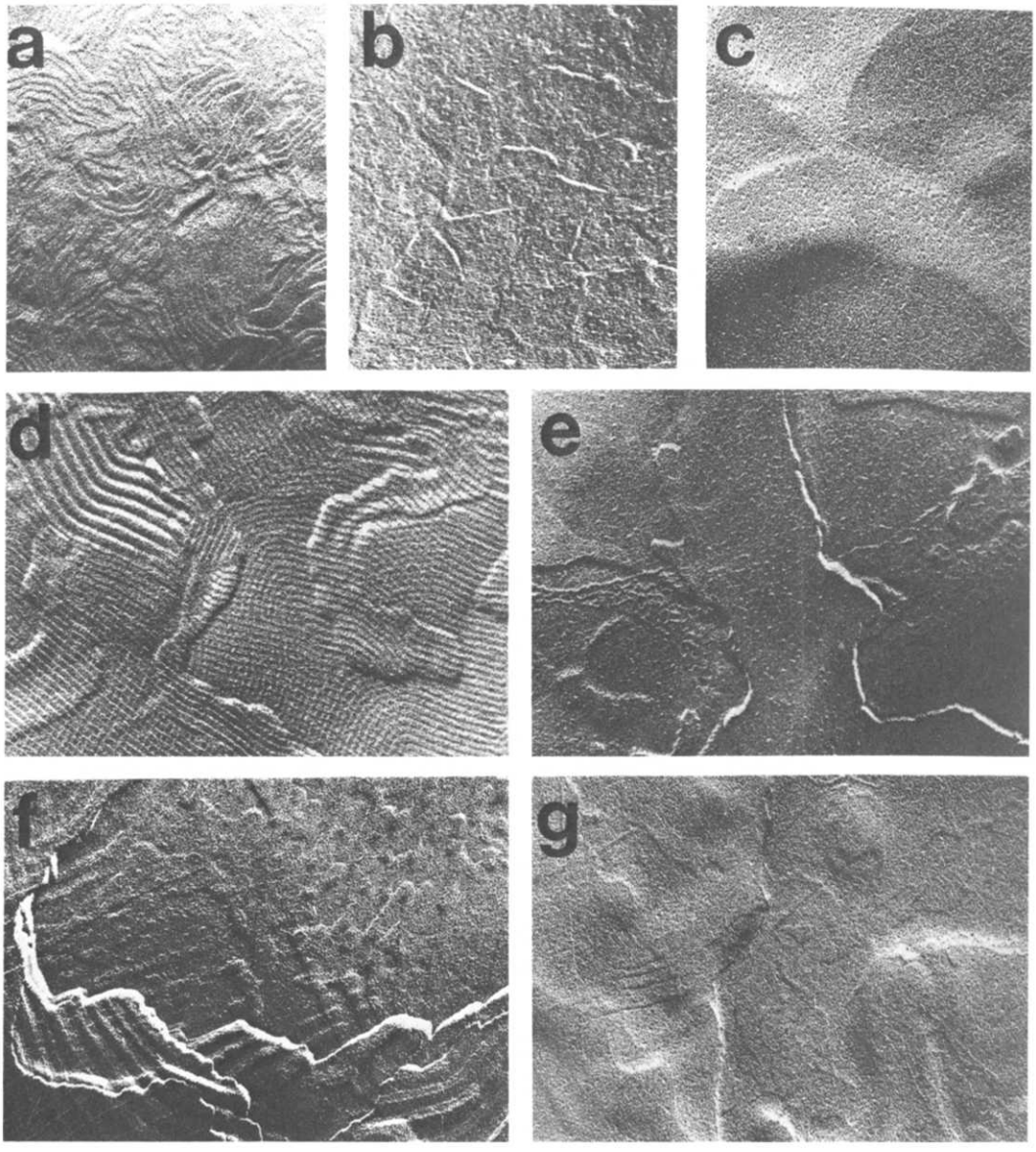


Fig. 5. Freeze-fracture electron micrographs of aqueous dispersions of dipalmitoyl phosphatidylcholine-dipalmitoyl phosphatidylserine mixtures. Mol% dipalmitoyl phosphatidylserine and quench temperature are as follows: a, 18%, 51°C; b, 57%, 53°C; c, 75%, 54°C; d, 18%, 43°C; e, 75%, 46°C; f, 18%, 37°C after cooling from 56°C; g, 18%, 36°C. All quench temperatures are ±2—3°C. Magnifications are about 44 000X.

## Discussion

The phase diagrams drawn in Figs. 2C and 4B for binary mixtures of dipalmitoyl phosphatidylcholine and dimyristoyl phosphatidylcholine with dipalmitoyl phosphatidylserine represent the best approximations to the spin-label and freeze-fracture data that are consistent with the (thermodynamic) rules for the

construction of phase diagrams [35,36]. Both of these phase diagrams show three 2-phase regions. The existence of these three 2-phase regions in the dimyristoyl phosphatidylcholine-dipalmitoyl phosphatidylserine phase diagram is clearly indicated by freeze-fracture electron microscopy (Fig. 3 c—f). Although less complete, freeze-fracture data obtained for dipalmitoyl phosphatidylcholine/dipalmitoyl phosphatidylserine mixtures also correlates quite well with the number and location of phases expected on the basis of the temperature-composition diagram (Fig. 4B). The only observed inconsistency between freeze-fracture data and our postulated phase diagrams occurs when samples containing 82 : 18 dipalmitoyl phosphatidylcholine : dipalmitoyl phoshatidylserine are quenched from 42—44°C (Fig. 5d). While the phase diagram leads us to expect a jumbled texture in equilibrium with either a smooth or banded texture, freeze-fracture repeatedly reveals banded fracture faces on samples quenched from this point. This inconsistency probably stems from the extremely narrow transition region and the 2—3°C inaccuracy in the freeze-fracture quench temperature.

Two features of the phase diagrams warrant special comment. The horizontal lines in Figs. 2C and 4B predict the existence of a temperature in each diagram at which all three phases, $L_\alpha$, $P_\beta'$, and $L_\beta'$, coexist for a range of lipid compositions. Consistent with this prediction, we observe three coexisting textures on the fracture faces of dimyristoyl phosphatidylcholine-dipalmitoyl phosphatidylserine (82 : 18) samples quenched from a temperature near that of the expected three-phase temperature (Fig. 6). The existence of three coexisting textures on fracture faces of this and other lipid mixtures is recorded at the appropriate points on the phase diagrams (Fig. 2C and 4B) by listing all three designating letters in decreasing order of dominance of the textures.

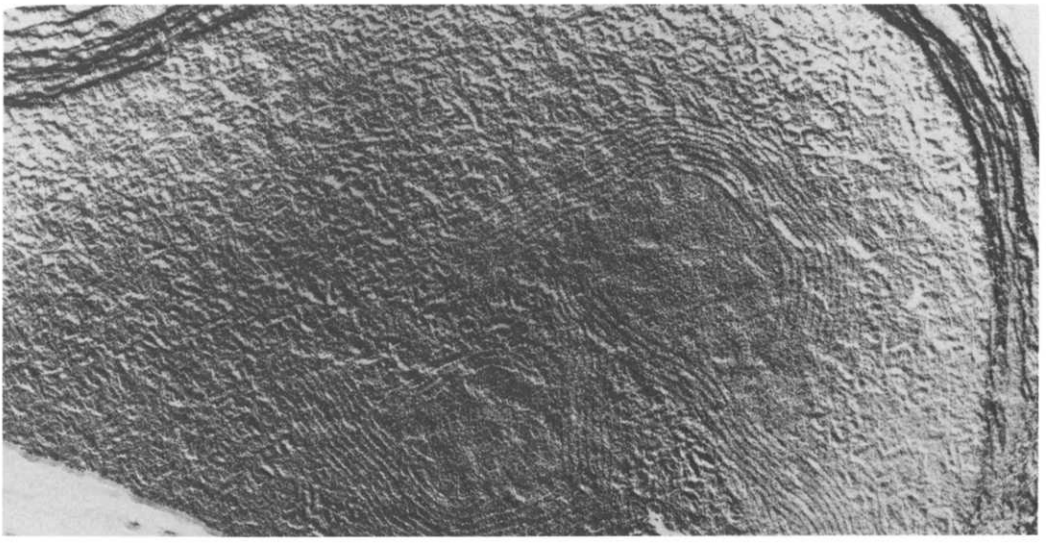

Fig. 6. Freeze-fracture electron micrograph of an aqueous dispersion of 82 : 18 dimyristoyl phosphatidylcholine:dipalmitoyl phosphatidylserine quenched from 35(±2)°C. Magnification is about 44 000X. Note the possibility of three distinct textures (phases).

The second point concerns the banding pattern seen in the microphotographs. Most microphotographs show domains having bands similar to those seen in the $P_{\beta'}$ phase of pure phosphatidylcholines (i.e., with periodicities of 100—400 Å), or domains having no bands at all. This, of course, is consistent with the reported phase diagrams. However, the reported phase diagrams do not preclude the theoretical possibility that, as the $P_{\beta'}$ phase becomes richer and richer in phosphatidylserine, the banding pattern might become weaker and weaker (bands of lower amplitude and/or larger wavelength). We believe that effects of this type could lead to second-order phase transitions in other lipid mixtures, an effect discussed in the Appendix.

In drawing the phase diagrams shown in Fig. 2C and 4B we have assumed that the low temperature phase of dipalmitoyl phosphatidylserine is $L_{\beta'}$ and that this phase is miscible with the low temperature phase $L_{\beta'}$ of the two phosphatidylcholines. From the present point of view it is not necessary to distinguish whether the low temperature phase of dipalmitoyl phosphatidylserine is $L_{\beta}$ or $L_{\beta'}$ as long as the crystallographic symmetry of this phase is the same as $L_{\beta'}$ for the phosphatidylcholines; otherwise additional phase boundaries would be observed.

Earlier correlations between spin-label TEMPO data and freeze-fracture electron microscopic data have been particularly simple for a number of binary mixtures of phosphatidylcholines [31,32]. This must be due in part to the fact that at least in some cases the $P_{\beta'}$ phase forms a complete range of solid solutions and is readily identified in the microphotographs. However, the recent observations that the banded $P_{\beta'}$ phase is stable over only a limited temperature range [22,37] indicates that it may be possible to include the lower as well as upper phase boundaries for the $P_{\beta'}$ phases in these binary mixtures throughout the composition ranges.

It is interesting to note that there are no features in these reported phase diagrams that obviously reflect the fact that the indicated lateral phase separations involve domains of different charge densities. However, solvent ionic strength, or pH, should modify these phase diagrams due to this lateral charge separation [4,6].

## Appendix

*Second-order phase transitions in lipid mixtures*

If one considers either of the two phase diagrams in Figs. 2C and 4B, it will be seen that any temperature-composition path leading from the $P_{\beta'}$ phase rich in a phosphatidylcholine to a $L_{\beta'}$ phase rich in phosphatidylserine leads either through a point representing a first-order phase transition or through a two-phase region. The vast majority of the microphotographs we have observed are consistent with these phase diagrams in that, when a single domain is observed, it is not banded, or the bands are in the range 100—400 Å.

In principle, however, it is possible to imagine a theoretical situation wherein the inclusion of a second lipid B in a solid solution of a first lipid A having a banded pattern, leads to a continuous disappearance of the bands, either through a diminishing band amplitude and/or increasing wavelength. Indeed, there are a number of freeze-fracture data in the literature to suggest this possi-

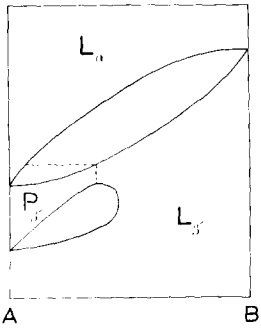


Fig. 7. A theoretical, speculative phase diagram illustrating the possibility that a homogeneous binary phase having one unique structure (the "banded" $P_{\beta}'$ phase) may change continuously through a second-order transition to a phase having a distinctly different structure (the "non-banded" $L_{\beta}'$ phase). The nearly vertical dotted line represents a second-order transition between the $P_{\beta}'$ phase (to the left of this line) and the $L_{\beta}'$ phase (on the dotted line, and to the right of this line). For a discussion of tricritical points see refs. 41—43.

bility [27,38] but none of these studies have been sufficiently extensive or appropriately designed to test this possibility.

A schematic phase diagram is represented in Fig. 7 wherein the dotted lines represent a second-order transition. Just to the left of the nearly vertical dotted line ($P_{\beta}'$ phase) we imagine the bands to be weak, and at and to the right of this dotted line ($L_{\beta}'$ phase) the bands are considered to be totally absent. One can easily see how the phase diagrams in Figs. 2C, 4B, and 7 can be looked upon as being extensions of one another and how, in fact, it might be difficult to distinguish, for example, the diagram in Fig. 2C from the diagram in Fig. 7 if the $P_{\beta}'$-$L_{\beta}'$ region were close but not touching the phase boundaries of the $L_{\alpha}$-$L_{\beta}'$ two-phase region.

## Acknowledgements

We are indebted to Stanford's Department of Biological Sciences for making their electron microscopy facilities available for this work, Mr. Robert Marshall for his assistance in their operation and Drs. Allan Campbell and Robert Simoni for the use of controlled-temperature rooms in their laboratories. We also thank Drs. Hans Andersen and G.M. Pound for helpful discussions. This research has been supported by the National Science Foundation Grant nos. BMS 75-02381 and BMS 75-02381 A01. It has benefited from facilities made available to Stanford University by the Advanced Research Projects Agency through the Center for Materials Research.

## References

1 Lansman, J. and Haynes, D. (1975) Biochim. Biopys. Acta 394, 335—347
2 Jacobson, K. and Papahadjopoulos, D. (1975) Biochemistry 14, 152—161
3 Ohnishi, S. (1976) in Advances in Biophysics (Kotani, M., ed.), Vol. 8, pp. 57—67, University of Tokyo Press, Tokyo
4 Träuble, H. (1977) Proceedings of Nobel Foundation Symposium 34, Structure of Biological Membranes (Abrahamsson, S. and Pascher, I., eds.), pp. 509—550, Plenum Press, new York

5 Marsh, D. (1976) VIIth International Conference on Magnetic Resonance in Biological Systems, Abstracts-Programme-Résumés, St. Jovite, Quebec, Canada, 146
6 Galla, H.J. and Sackmann, E. (1975) Biochim. Biophys. Acta 401, 509–529
7 Birrell, G.B. and Griffith, O.H. (1976) Biochemistry 15, 2925–2929
8 Linden, C.D., Wright, K.L., McConnell, H.M. and Fox, C.F. (1973) Proc. Natl. Acad. Sci. U.S. 70, 2271–2275
9 Linden, C.D. and Fox, C.F. (1973) J. Supramol. Struct. 1, 535–544
10 Papahadjopoulos, D., Jacobson, K., Nir, S. and Isac, T. (1973) Biochim. Biophys. Acta 311, 330–348
11 Wu, S.H.W. and McConnell, H.M. (1973) Biochem. Biophys. Res. Commun. 55, 484–491
12 Marsh, D., Watts, A. and Knowles, P.F. (1976) Biochemistry 15, 3570–3578
13 Kleemann, W. and McConnell, H.M. (1976) Biochim. Biophys. Acta 419, 206–222
14 Sharom, F.J. and Grant, C.W.M. (1975) Biochem. Biophys. Res. Commun. 67, 1501–1506
15 Breisblatt, W. and Ohki, S. (1976) J. Membrane Biol. 29, 127–146
16 Papahadjopoulos, D., Vail, W.J., Pangborn, W.A. and Poste, G. (1976) Biochim. Biophys. Acta 448, 265–283
17 Luzzati, V. and Tardieu, A. (1974) in Annual Review of Physical Chemistry (Eyring, H., Christensen, C.J. and Johnston, H.S., eds.), Vol. 25, pp. 79–94
18 Trudell, J.R., Hubbell, W.L. and Cohen, E.N. (1973) Biochim. Biophys. Acta 291, 321–327
19 Nagle, J.F. (1973) Proc. Natl. Acad. Sci. U.S. 70, 3443–3444
20 Mabrey, S. and Sturtevant, J.M. (1976) Proc. Natl. Acad. Sci. U.S. 73, 3862–3866
21 Gaffney, B.J. and Chen, S. (1976) in Methods in Membrane Biology (Korn, E.D., ed.), Vol. 8, pp. 291–358, Plenum Publishing Corporation, New York
22 Luna, E.J. and McConnell, H.M. (1977) Biochim. Biophys. Acta 466, 381–392
23 Landau, L.D. and Lifskitz, E.M. (1969) Statistical Physics (Vol. 5 of Course of Theoretical Physics), pp. 424–454, Addison-Wesley Publishing Company, London
24 Baer, E. and Maurukas, J. (1955) J. Biol. Chem. 212, 25–38
25 McClare, C.W.F. (1971) Anal. Biochem. 39, 527–530
26 Gaffney, B.J. (1974) in Methods in Enzymology (Fleischer, S. and Packer, L., eds.), Vol. XXXII, Part B, pp. 161–197
27 Kleemann, W. and McConnell, H. (1974) Biochim. Biophys. Acta 345, 220–230
28 Shimshick, E. and McConnell, H. (1973) Biochemistry 12, 2351–2360
29 Wu, S. and McConnell, H.M. (1975) Biochemistry 14, 847–854
30 MacDonald, R.C., Simon, S.A. and Baer, E. (1976) Biochemistry 15, 885–891
31 Grant, C.W.M., Wu, S.H.W. and McConnell, H.M. (1974) Biochim. Biophys. Acta 363, 151–158
32 Kleemann, W., Grant, C.W.M. and McConnell, H.M. (1974) J. Supramol. Struct. 2, 609–616
33 Pinto da Silva, P. (1971) J. Microscopie 12, 185–192
34 Ververgaert, P.H.J., Verkleij, A.J., Verhoeven, J.J. and Elber, P.F. (1973) Biochim. Biophys. Acta 311, 651–654
35 Gordon, P. (1968) Principles of Phase Diagrams in Materials Systems, pp. 186–191, McGraw-Hill Book Company, New York
36 Rhines, F.N. (1956) Phase Diagrams in Metallurgy (Metallurgy and Metallurgical Engineering Series) pp. 101–105, McGraw-Hill Book Company, New York
37 Janiak, M.J., Small, D.M. and Shipley, G.G. (1976) Biochemistry 15, 4575–4580
38 Verkleij, A.J. and Ververgaert, P.H.J.Th. (1975) in Annual Review of Physical Chemistry (Eyring, H., Christensen, C.J. and Johnston, H.S., eds.), Vol. 26, pp. 101–122
39 Griffith, O.H., Jost, P.C. and McConnell, H.M. (1976) Spin Labeling; Theory and Applications, Academic Press, New York
40 Träuble, H. and Eibl, H. (1974) Proc. Natl. Acad. Sci. U.S. 71, 214–219
41 Griffiths, R.B. (1970) Phys. Rev. Lett. 24, 715–717
42 Ahlers, G. (1974) in The Physics of Liquid and Solid Helium (Ketterson, J.B. and Bennemann, K.H., eds.), chap. 8, Wiley and Sons, New York
43 Landau, D.P., Keen, B.E., Schneider, B. and Wolf, W.P. (1971) Phys. Rev. B 3, 2310–2343